Supplementary Material (ESI) for RSC Advances
This journal is © The Royal Society of Chemistry 2013

Supplementary Information

Controlled chemistry in tailored graphene nanoribbons for electrochemistry: a rational approach to optimizing molecule detection.

Aida Martín[a], *Javier Hernández-Ferrer*[b], *Luis Vázquez*[c], *María Teresa Martínez*[b] *and Alberto Escarpa**[a]

Supplementary Material (ESI) for RSC Advances
This journal is © The Royal Society of Chemistry 2013

OPTIMIZATION OF THE GNRred DISPERSION

Strong sonication of the GNRred solution was required for obtaining a high signal intensity and rapid electron transfer between the analyte and electrode surface, as shown in **Fig. S1.** A GNRred dispersion prepared without tip sonication tended to form accumulated graphene mass piles on the electrode surface, which increased the resistivity and decreased the current. By contrast, tip sonication tremendously improved the dispersion properties, and the solution deposited a thin film on the electrode. The electrons then had to travel through only a few layers, and the conductivity of the electrode remained high. Excellent electrochemical responses were achieved using tip-sonicated GNRred solutions.

GNRox is more insulating than GNRred because the lower sp^2 content. Strong sonication of the dispersion did not improve the electrochemical responses because the electrons inherently faced greater barriers in migrating through the GNRox lattice. The electrode responses before and after sonication were indistinguishable.

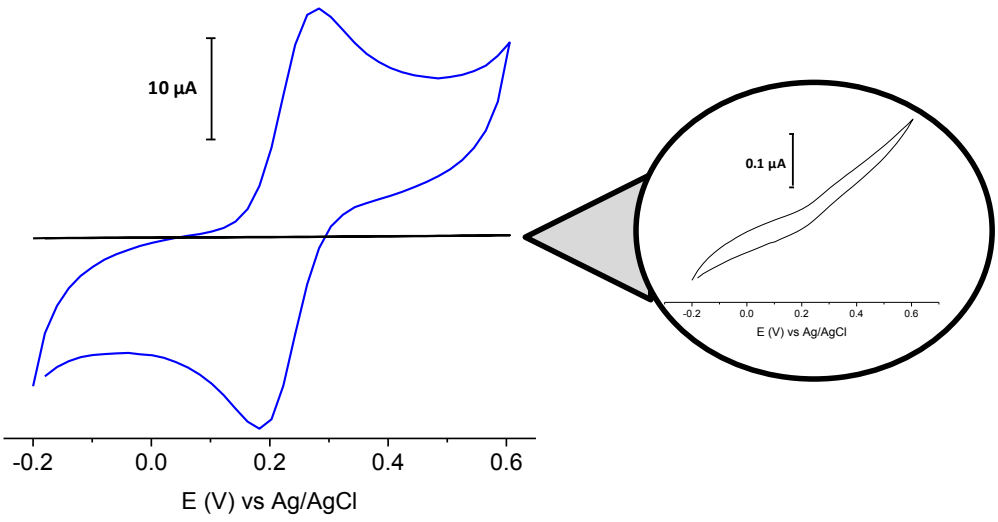

Fig. S1. Cyclic voltammetry of the GNR materials dispersed without (black) or with tip sonication (blue). The working electrolyte was 1 mM $K_3[Fe(CN)_6]$ in 0.1 M PBS. The right-hand panel shows a magnified view of the black line shown in the left-hand panel.

Supplementary Material (ESI) for RSC Advances
This journal is © The Royal Society of Chemistry 2013

OPTIMIZATION OF GCE CASTING WITH GNRs

The material deposited on the electrode surface was quantified by depositing different concentrations of the graphene material. The optimized deposition parameters were selected with consideration for both the quality of the dispersion (the absence of mass deposits) and the quality of the resulting signal.

Table S1. Cathodic current intensities in the CV study of 1 mM $[Ru(NH_3)_6]^{3+}$ in 1 M KCl, using the GNRox/GC-modified electrodes prepared by depositing different volumes of a 0.5 mg/mL graphene dispersion.

Volume (µL)	**0**	**1**	**5**	**10**	**20**
i_{cat} (µA)	–6.2	–8.7	–11.7	–21.8	–24.1
RSD (%, n=3)	2.0	0.6	2.4	3.3	3.6

Supplementary Material (ESI) for RSC Advances
This journal is © The Royal Society of Chemistry 2013

ANALYTICAL CHARACTERIZATION OF THE GNRs BY XRD

The XRD data obtained from the MWCNTs, GNRox, and GNRred samples are plotted in **Fig. S2**. The two-theta angles observed for each material were characteristic of a pattern and implied the presence of distinct structures.

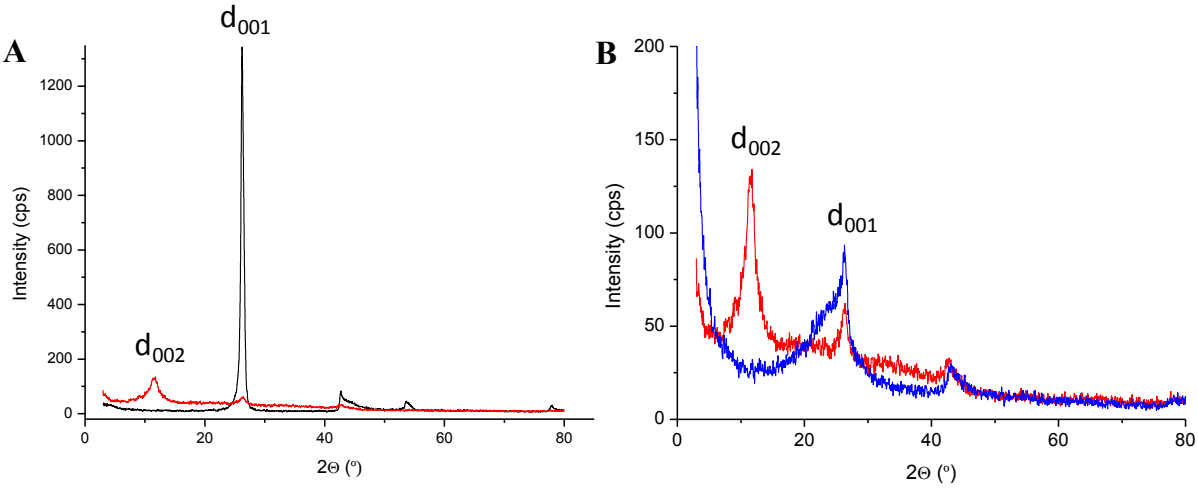

Fig. S2. X-ray diffractograms for the MWCNTs (black) and GNRox (red) (scale x5 in GNRox) **(A)**, and GNRox (red) and GNRred (blue) **(B)**.

Supplementary Material (ESI) for RSC Advances
This journal is © The Royal Society of Chemistry 2013

ANALYTICAL CHARACTERIZATION OF THE GNRs BY RAMAN SPECTROSCOPY

Raman spectra of the MWCNTs, GNRox, and GNRred are showed in **Fig. S3**.

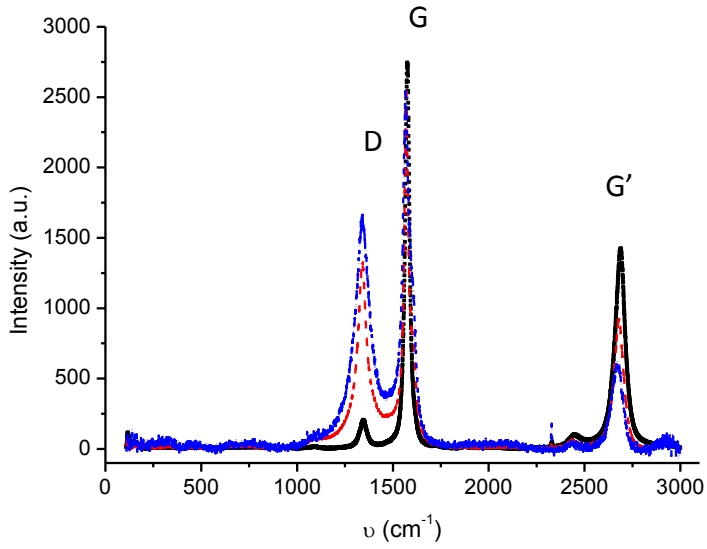

Fig. S3. Raman spectra of the MWCNTs (black), GNRox (red), and GNRred (blue). The scale of the GNRred sample is 10x the scale of the other sample spectra.

Supplementary Material (ESI) for RSC Advances
This journal is © The Royal Society of Chemistry 2013

ANALYTICAL CHARACTERIZATION OF THE GNRs BY XPS

XPS data obtained from the GNRox and GNRred are showed in **Fig. S4**. The GNRox sample had a low sp^2 carbon content and a high number of oxygen groups. The GNRred sample displayed a higher atomic percentage of sp^2 carbon atoms, and the presence of C-N bonds was significant due to the reduction reaction with hydrazine.

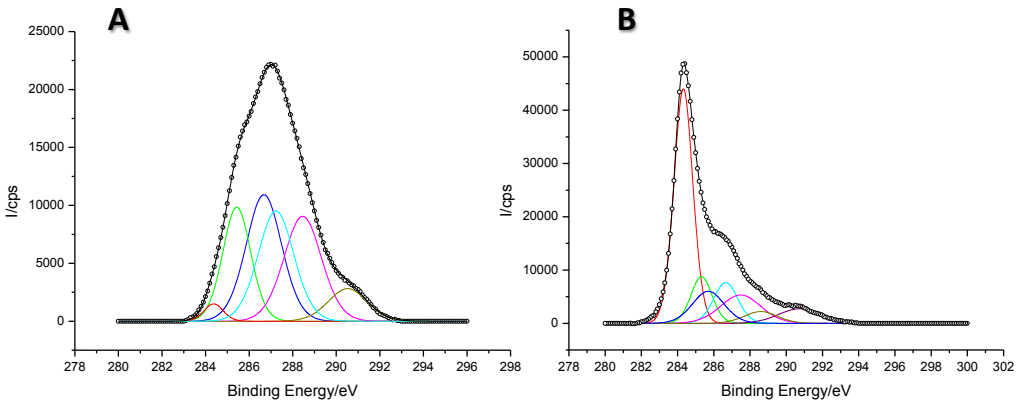

C

GNRox	Binding energy (eV)	% atomic	GNRred	Binding energy (eV)	% atomic
C-sp^2	284,4	1,94	C-sp^2	284,3	46,52
C-sp^3	285,4	18,60	C-sp^3	285,4	10,22
Carboxyl	288,5	22,94	Carboxyl	288,3	4,08
Ketone and aldehyde	287,2	22,99	Ketone and aldehyde	287,5	11,91
Alcohol, epoxy, ether	286,95	26,19	Alcohol, epoxi, éter	286,7	10,29
π-π*	290,65	7,35	π-π*	290,7	6,26
			C-N	285,7	10,63

Fig. S4. C1s XPS spectra obtained from the GNRox (**A**) and GNRred (**B**) samples, recorded with a photon energy of hν = 400 eV. Table of the binding energies and atomic percentages estimated from the XPS spectra provided in A and B, for GNRox and GNRred, respectively (**C**).

Supplementary Material (ESI) for RSC Advances
This journal is © The Royal Society of Chemistry 2013

ANALYTICAL CHARACTERIZATION OF THE GNRs BY FT-IR

IR spectroscopy permits an analysis of the functional moieties present in the GNRs. **Fig. S5** shows the sp^2-carbon vibrational bands obtained from the MWCNTs (**A**). The GNRox spectra indicated the presence of oxygen moieties due to carboxyl, epoxyl, and hydroxyl groups (**B**). The GNRred spectrum shows the remained oxygen moiety signals between 1400 and 1700 cm^{-1}, however, the vibrations corresponding to the C-O stretch between 1250 and 1000 cm^{-1} were reduced to a greater extent, as compared to the GNRox spectrum. Vibrations at 3200 cm^{-1} due to the C-N bonds arose from the chemical reduction step (**C**). The GNRred spectrum displayed a lower band intensity compared to the GNRox spectrum, confirming that the oxygen moieties had been reduced. These results were consistent with the Lerf–Klinowsky model.

IR spectroscopy is not a quantitative technique, unlike XPS or measurements of the total oxygen content. As a result, IR spectroscopy can only corroborate data obtained using other means.

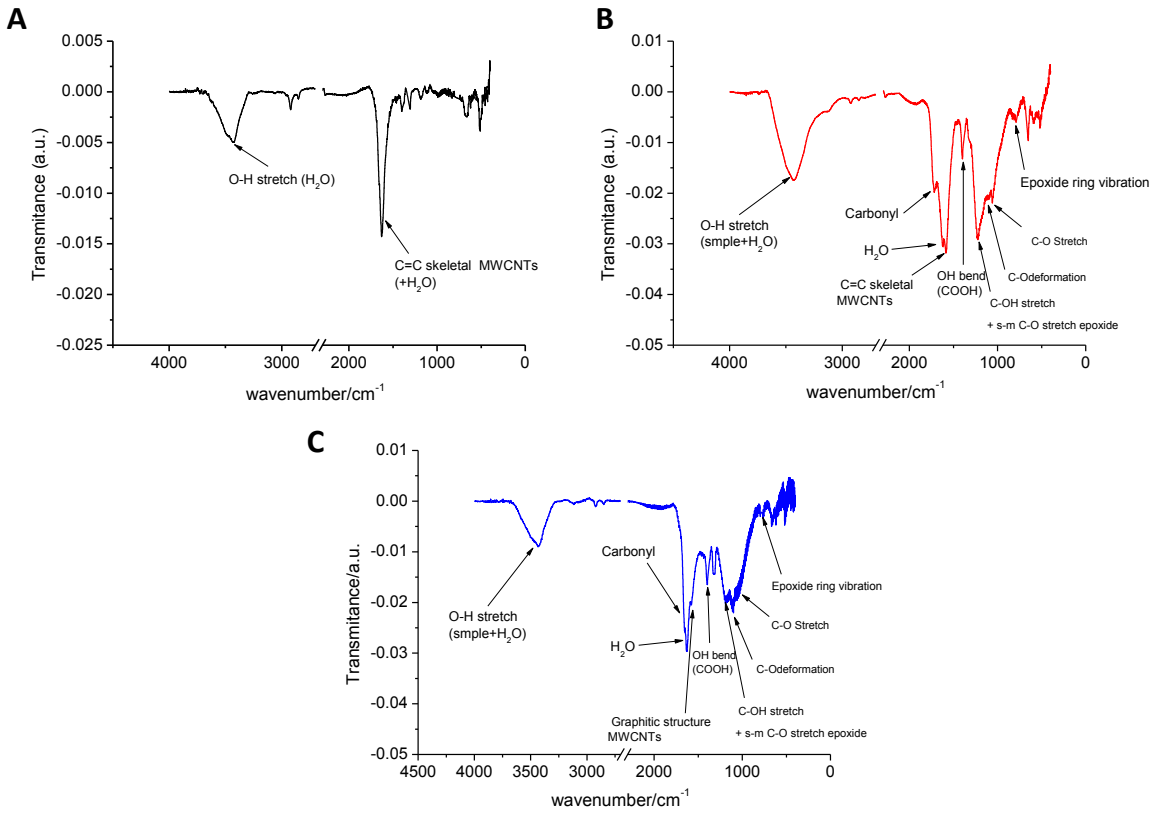

Fig. S5. IR spectra of the MWCNTs (**A**), GNRox (**B**), and GNRred (**C**) samples.

Supplementary Material (ESI) for RSC Advances
This journal is © The Royal Society of Chemistry 2013

EVALUATION OF THE ELECTROCHEMICAL AREAS OF THE GNR-MODIFIED ELECTRODES

The electrode surface area available for redox reactions was assessed based on chronocoulometric charge-time plots for the reduction of potassium hexacyanoferrate (III) and the corresponding linear fits for Q vs $t^{1/2}$, as shown in **Fig. S6**. Within 1 s, the chronocoulometric charge-time plots reached a plateau during the reduction of potassium hexacyanoferrate (III). The slopes of the plots of Q vs. $t^{1/2}$, obtained by chronocoulometry, were obtained as follows: 5.8 x 10^{-6}, 9.6 x 10^{-6}, 1.7 x 10^{-5}, and 3.5 x 10^{-5} $Cs^{-1/2}$ for, respectively, the bare GCE, MWCNTs/GCE, GNRox/GCE and GNRred/GCE. These values yielded estimates for the electrochemical areas: 0.030, 0.071, 0.113, and 0.267 cm^2, respectively.

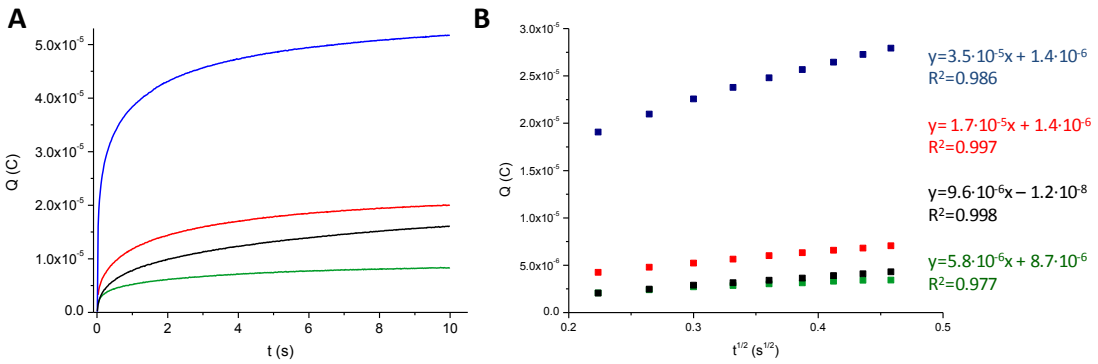

Fig. S6. (A) Chronocoulometric charge-time plots for the reduction of 0.45 mM $K_3[Fe(CN)_6]$ in 0.1 M PBS (pH=7.4). GCE (green), GCE/MWCNTs (black), GCE/GNRox (red), and GCE/GNRred (blue). (**B**) Chronocoulometric plots of the charge versus $t^{1/2}$ and linear fits for GCE (black), GCE/MWCNTs (green), GCE/GNRox (red), and GCE/GNRred (blue).

Supplementary Material (ESI) for RSC Advances
This journal is © The Royal Society of Chemistry 2013

VOLTAMMETRY OF THE BENZENEDIOL ISOMERS

Table S2. Oxidation potentials and peak intensities for hydroquinone (HQ), catechol (CT), and resorcinol (RS). The brackets indicate the RSD values (%, n=3 electrodes).

Variable	Electrodic material	HQ	CT	RS
E (V)	Bare GCE	0.178 (1.6)	0.137 (2.1)	0.530 (2.1)
	MWCNTs	0.107 (1.3)	0.228 (1.3)	0.495 (2.6)
	GNRox	0.027 (0)	0.243 (1.6)	0.505 (2.0)
	GNRred	0.032 (0)	0.142 (1.2)	0.369 (1.0)
I_p (μA)	Bare GCE	10.0 (2.9)	6.2 (3.9)	5.61 (6.0)
	MWCNTs	15.1 (2.3)	12.0 (3.6)	11.4 (6.7)
	GNRox	26.1 (0.7)	6.5 (4.6)	22.5 (8.4)
	GNRred	212.0 (1.1)	111.0 (5.8)	32.1 (5.7)

VOLTAMMETRY OF AA, LD, AND UA

Table S3. Oxidation potentials and peak intensities for ascorbic acid (AA), levodopa (LD), uric acid (UA), and tyrosine (L-Tyr). The brackets indicate the RSD values (%, n=3 electrodes).

Variable	Electrodic material	AA	LD	UA	L-Tyr
E (V)	Bare GCE	0.465 (0.7)	0.404 (2.0)	0.493 (1.2)	0.745 (1.0)
	MWCNTs	0.273 (1.2)	0.319 (0.5)	0.359 (1.5)	0.580 (0.4)
	GNRox	0.142 (1.1)	0.186 (3.0)	0.278 (1.6)	0.575 (0.7)
	GNRred	–0.054 (1.2)	0.130 (1.0)	0.257 (1.0)	0.535 (2.0)
I_p (μA)	Bare GCE	0.9 (9)	3.3 (10.1)	3.7 (4.1)	1.4 (1.4)
	MWCNTs	4.3 (3.7)	4.0 (1.3)	8.0 (3.4)	12.5 (8.0)
	GNRox	2.3 (5.0)	15.3 (8.6)	41.3 (6.5)	16.4 (6.1)
	GNRred	9.4 (4.0)	33.9 (2.4)	44.1 (4.0)	32.8 (1.5)

Supplementary Material (ESI) for RSC Advances
This journal is © The Royal Society of Chemistry 2013

VOLTAMMETRY OF THE TARGET MOLECULES IN COMPLEX SAMPLES.

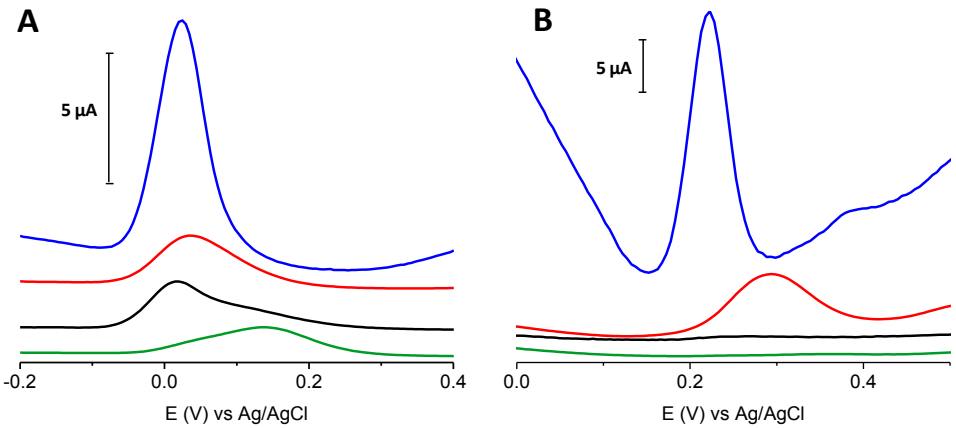

Fig. S7. Differential pulse voltammograms for the detection of HQ in a cosmetic sample **(A)** and UA in a urine sample **(B),** on (—) Bare GCE, (—) MWCNTs, (—) GNRox, and (—) GNRred electrodes.